Phys. Med. Biol. **45** (2000) 529–539. Printed in the UK PII: S0031-9155(00)06526-X

# Physical properties of hydrated tissue determined by surface interferometry of laser-induced thermoelastic deformation

Marta L Dark†§, Lev T Perelman†, Irving Itzkan†, Jonathan L Schaffer†‡ and Michael S Feld†

† Laser Biomedical Research Center, G R Harrison Spectroscopy Laboratory, MIT, 77 Massachusetts Avenue, Room 6-014, Cambridge, MA 02139, USA
‡ Department of Orthopaedic Surgery, Brigham and Women's Hospital, Harvard Medical School, 75 Francis Street, Boston, MA 02115, USA

E-mail: mldark@alum.mit.edu

Received 2 August 1999, in final form 21 October 1999

**Abstract.** Knee meniscus is a hydrated tissue; it is a fibrocartilage of the knee joint composed primarily of water. We present results of interferometric surface monitoring by which we measure physical properties of human knee meniscal cartilage. The physical response of biological tissue to a short laser pulse is primarily thermomechanical. When the pulse is shorter than characteristic times (thermal diffusion time and acoustic relaxation time) stresses build and propagate as acoustic waves in the tissue. The tissue responds to the laser-induced stress by thermoelastic expansion. Solving the thermoelastic wave equation numerically predicts the correct laser-induced expansion. By comparing theory with experimental data, we can obtain the longitudinal speed of sound, the effective optical penetration depth and the Grüneisen coefficient. This study yields information about the laser–tissue interaction and determines properties of the meniscus samples that could be used as diagnostic parameters.

## 1. Introduction

The knee is an important diarthrodial joint, allowing people to function in their daily lives but causing potentially significant pain and inconvenience when the knee cartilage is dysfunctional, such as from injury related tears or degenerative changes. There are two menisci within the knee joint. They are crescent-shaped tissues with a wedge-shaped cross section, located between the tibial plateau and the femoral condyle (Bullough 1992). Meniscal cartilage is a fibrous cartilage that absorbs shock, increases lubrication and transmits load across the knee joint (Ghosh and Taylor 1987). Its fibrous extracellular matrix is composed mainly of collagen fibres, with water comprising 70–75% of its total weight. The dry weight consists of approximately 75% collagen, 8–13% non-collagen proteins and 1% hexosamine (Adams and Hukins 1992).

An important step in deciding whether or not lasers can be used as diagnostic tools is to determine the behaviour and physical properties of these tissues following laser irradiation. We wish to determine if measurements of certain properties of menisci are capable of distinguishing between normal tissue and tissue with degenerative changes. Such a method might provide orthopaedic surgeons with a more precise manner of guiding cutting and cartilage removal.

§ Present address: Center for Bio-Molecular Science and Engineering, Naval Research Laboratory, Code 6950, 4555 Overlook Avenue SW, Washington, DC 20375, USA.

0031-9155/00/020529+11$30.00  

When a tissue sample absorbs a laser pulse of short duration, a non-zero temperature distribution is created. If the laser pulse duration, $\tau_p$, is shorter than both the acoustic relaxation and thermal relaxation times, then the system is mechanically and thermally confined. The acoustic relaxation time is $1/\mu_{\text{eff}} c_L$, and the thermal relaxation time is $a/\kappa\mu_{\text{eff}}^2$, where $\mu_{\text{eff}}$ is the effective attenuation coefficient, $c_L$ the longitudinal sound speed, $\kappa$ the thermal diffusivity and $a$ a numerical constant dependent on geometry of the problem and of the order of unity. Photomechanical processes will dominate the laser–tissue interaction. The resulting temperature distribution creates internal stresses, which propagate as acoustic waves. In a liquid such as water, only longitudinal waves will propagate. Thus, we expect little or no transverse wave propagation in hydrated tissue since it is composed mostly of water. The material responds to these stresses through thermoelastic deformations, which can be described by the thermoelastic wave equation (Itzkan *et al* 1995). Other researchers have used video techniques and time-resolved detection of stresses to study laser-induced behaviours of tissue substitutes, such as gelatin and aqueous dye (Paltauf and Schmidt-Kloiber 1996, Oraevsky *et al* 1996).

We used an interferometric technique (Albagli *et al* 1994a) to measure surface expansion of human knee meniscus following its absorption of an 8 ns laser pulse. Our apparatus is similar to an interferometer recently described by Yablon and co-workers (Yablon *et al* 1999) used to determine absorption coefficients of cornea and water. However, they studied laser–tissue interactions that are thermally but not mechanically confined. Comparisons of our interferometric measurements with theoretical predictions obtained by solving the thermoelastic wave equation allow determination of the physical properties of meniscus. This method allows measurement of the longitudinal speed of sound, effective optical penetration depth and the Grüneisen coefficient. Such a technique is useful to determine physical properties of soft biological tissue on a microscopic scale.

## 2. Methods

### *2.1. Experiment*

A pump–probe interferometric technique developed by this research group was used to measure laser-induced surface expansion, and is described in a previous publication (Schaffer *et al* 1995). This technique measures surface expansion of a sample with spatial resolution of approximately 4 nm and temporal resolution of 3 ns. A schematic diagram of the experiment is given in figure 1.

The pump laser pulse is provided by a frequency-tripled $Q$-switched Nd:YAG laser (Continuum, NY-61, Santa Clara, CA) at a wavelength $\lambda$ of 354.7 nm and pulse duration $\tau_p = 8$ ns. The beam passes through a 3 mm aperture, and is focused to a 1 mm diameter spot on the sample's surface with a top-hat profile. A glan polarizing prism following the aperture modulates the energy per pulse (directed transversely to the tissue surface) between 0.4 to 10 mJ. Energy per pulse is measured with a laser beam analyser (Beam View Analyzer, Big Sky, MT).

The interferometric probe light from a cw He–Ne laser (Melles Griot, 05-LHP-926, Carlsbad, CA) is electronically shuttered to a 6 ms duration. A 50/50 beamsplitter is used in a Michelson interferometer set-up. A 5 cm lens focuses the light onto the target in the sample arm. The small fraction of light reflected from the air–target interface is recollimated by the lens and returned to the beamsplitter. A rotating corner cube ($f = 10$ Hz) in the reference arm moves into the beam path every 100 ms, and the interferometer is aligned for about 1 ms. The reference arm path length changes at a constant rate, creating an interference fringe pattern. The sample's motion modulates the frequency of the fringe pattern, and one can determine the direction and speed of the sample surface.

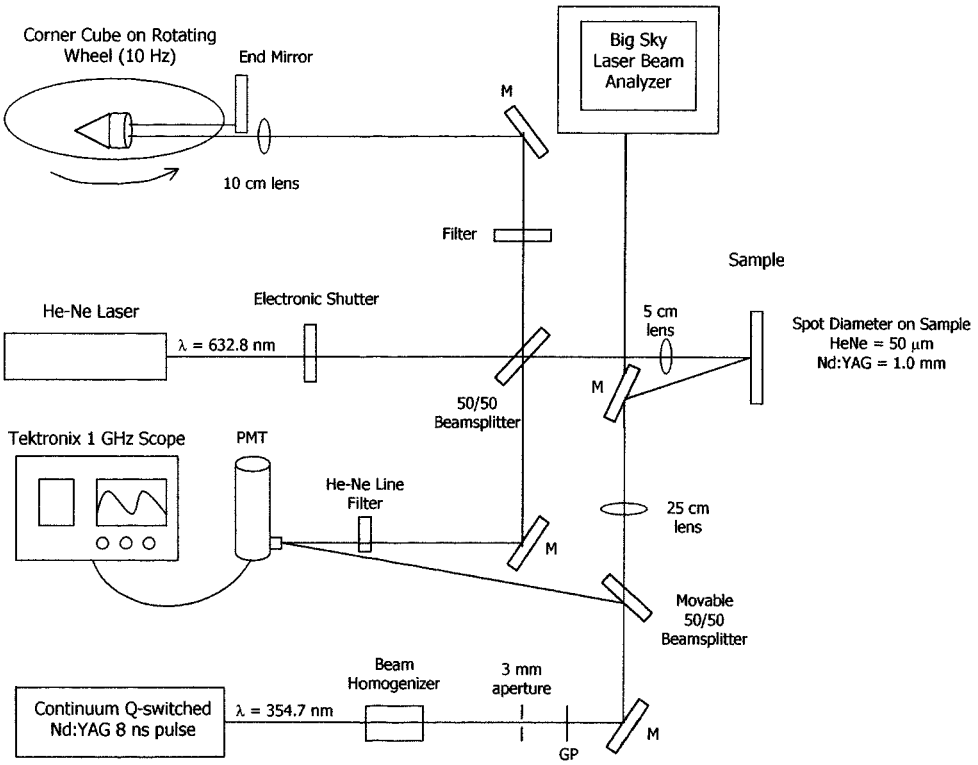


**Figure 1.** Schematic diagram of the laser surface interferometric apparatus: M, mirror; GP, Glan polarizer.

The light from both arms of the interferometer is combined by the beamsplitter and directed towards a red-sensitive photomultiplier (PMT) tube (Hammamatsu, R928, Japan). The PMT signal is captured and digitized at a rate of 1 gigasample/sec by a digital oscilloscope (Tektronix, DSA 601A, Beaverton, OR) and transferred to a computer for analysis. Data are collected for a 10 $\mu$s period, with the Nd:YAG pulse firing exactly 2 $\mu$s into this period (with a jitter of $\pm 2$ ns). A small portion of the Nd:YAG beam is directed to the PMT to ensure firing at 2 $\mu$s. Once correctly triggered we remove the beamsplitter, which directs Nd:YAG light to the PMT.

Experiments were performed on gelatin (Sigma, G 6650, Saint Louis, MO), and human knee meniscus. Meniscal tissue was obtained from patients undergoing total knee replacement surgery under an Internal Review Board (IRB) approved protocol. Samples were placed in normal saline for transport to the laboratory. They were then placed in a refrigerator at 4 °C and kept until use, which was within 24–30 h. Sites with sufficient interferometric signal were irradiated typically with five laser pulses of different energy values. We used pulse energies below ablation threshold, in order to avoid damaging the sample. Following irradiation, irradiated sites were marked with tissue marking dye (Bradley Products, Bloomington, MN), fixed in 10% formalin and prepared for a histological assessment.

### *2.2. Theory*

A theoretical model based on the theory of elasticity was developed to describe the time-dependent deformations of a hydrated tissue, such as meniscus, following absorption of a short

laser pulse. A numerical time-dependent solution of the thermoelastic wave equation has been obtained for laser-induced heating of a hydrated sample in a three-dimensional cylindrically symmetric geometry. This solution shows that the sample will undergo thermoelastic expansion and the surface will reach a new equilibrium position. The time constant of this expansion is governed by the ratio of the 1/e depth of laser light absorption, to the speed of sound in the sample, $1/\mu_{\text{eff}}c_L$.

The initial light distribution can be approximated by an exponentially decaying profile with tissue depth ($z > 0$), and a radial profile $L(r)$ dependent on the laser profile; $I(r, z) \backsimeq I_0 L(r) \exp(-\mu_{\text{eff}} z)$. In a turbid medium such as tissue, light is subject to both absorption and scattering. The effective penetration depth defined by transport theory is

$$D_{\text{eff}} = \frac{1}{\mu_{\text{eff}}} = \frac{1}{[3\mu_a(\mu_a + \mu_s')]^{1/2}} \tag{1}$$

where $\mu_a$ and $\mu_s'$ are the absorption and reduced scattering coefficients of transport theory (Star 1995). We can approximate the three-dimensional temperature distribution in our model that attenuates with an effective penetration depth to be

$$T_L(r, z) \backsimeq T_0 \exp(-\mu_{\text{eff}} z) L(r) \qquad \text{and} \qquad T_0 = \frac{\Phi \mu_a}{\rho C_V} \tag{2}$$

where $C_V$ is heat capacity (constant volume), $\Phi$ is laser fluence (energy per area) and $\rho$ is mass density. This approximation of temperature distribution is sufficient for our numerical model.

The non-zero temperature distribution result in internal stresses that lead to thermoelastic deformation. This deformation in a solid body is determined by the thermoelastic wave equation (Landau and Lifshitz 1986)

$$\rho \frac{\partial^2 \boldsymbol{u}}{\partial t^2} - \frac{E}{2(1+\nu)} \nabla^2 \boldsymbol{u} - \frac{E}{2(1+\nu)(1-2\nu)} \nabla(\nabla \cdot \boldsymbol{u}) = \frac{-E\beta}{3(1-2\nu)} \nabla T_L \tag{3}$$

subject to the appropriate initial and boundary conditions, where $\boldsymbol{u}$ is the displacement vector, $E$ is Young's modulus, $\nu$ is Poisson's ratio, $\beta$ is the thermal expansion coefficient and $T_L$ is the laser-induced temperature increase above a uniform ambient level. The wave equation is determined from Newton's second law, there the internal stress force is set equal to the product of acceleration and density. The stress tensor $\sigma_{ik}$ is defined as

$$\sigma_{ik} = \frac{E}{1+\nu} \left( u_{ik} + \frac{\nu}{1-2\nu} u_{jj} \delta_{ik} \right) - \frac{E\beta T_L}{3(1-2\nu)} \delta_{ik} \tag{4}$$

where $u_{ik}$ are components of the strain tensor (Landau and Lifshitz 1986).

We must solve these equations for a hydrated tissue, with high water content. For a liquid with a shear modulus of zero, Poisson's ratio approaches $\nu \to \frac{1}{2}$, and this value will be used for all calculations of meniscus (and gelatin) displacement. We can rewrite equation (3) using the definitions of longitudinal ($c_L$) and transverse ($c_T$) speed of sound:

$$\frac{\partial^2 \boldsymbol{u}}{\partial t^2} - c_L^2 \nabla^2 \boldsymbol{u} - \frac{c_T^2}{2(1-\nu)} \nabla(\nabla \cdot \boldsymbol{u}) = -\frac{c_L^2(1+\nu)}{3(1-\nu)} \beta \nabla T_L. \tag{5}$$

Longitudinal and transverse speeds of sound are (Landau and Lifshitz 1986) respectively

$$c_L^2 = \frac{E(1-\nu)}{\rho(1+\nu)(1-2\nu)} \qquad \text{and} \qquad c_T^2 = c_L^2 \frac{(1-2\nu)}{2(1-\nu)}. \tag{6}$$

The transverse sound speed equals zero in a liquid; thus, the third term on the left-hand side of equation (5) vanishes.

### *2.3. Numerical solution*

We have a numerical model that solves the thermoelastic wave equation (5) as a function of time and space in cylindrical coordinates (Albagli 1994). We have an axially symmetric geometry. On a two-dimensional grid $(r, z)$, we calculate variables such as components of stress, acceleration and velocity at each grid point. From the stress components acceleration can be determined, as the internal stress equals acceleration multiplied by density. Using the Adams–Bashforth time-stepping method (Potter 1977), acceleration is integrated twice to obtain displacement as a function of time and position.

After the transient stresses have passed, the material attains quasi-steady state equilibrium and will remain in this deformed state until thermal diffusion occurs. We have found an expression for the equilibrium surface displacement on axis $u(r = 0, z = 0, t > 1/\mu_{\text{eff}} c_L)$, a value that can be compared with experimental measurements (Albagli *et al* 1994b). In terms of laser fluence $\Phi$, equilibrium surface displacement on-axis $u(r = 0, z = 0)$ becomes

$$u(0, 0, t > 1/\mu_{\text{eff}} c_L) = S_0 = \frac{2(1+\nu)}{3} \frac{\beta}{\rho C_V} g_0(R)\Phi \tag{7}$$

where $1/\mu_{\text{eff}} c_L$ is the acoustic relaxation time, the function $g_0(R)$ is a geometrical correction factor that describes the significance of aspect ratio $R = w/D_{\text{eff}}$ and $w$ is the beam radius. We obtain the correction factor as part of solving for axial surface displacement at long times ($t \rightarrow \infty$), and it includes a first-order Bessel function (Albagli 1994). For large $R$, a pancake geometry, $g_0(R)$ approaches 1. For a long cylinder ($R < 1$), $g_0(R)$ goes to zero. For meniscus, where $1.8 \leqslant R \leqslant 2.3$, the correction factor is $0.61 \leqslant g_0(R) \leqslant 0.67$ (Dark 1999).

Figure 2 shows the time-dependent surface displacement predicted by the numerical model for a hydrated sample. As described earlier, the irradiated volume of the tissue is modelled as a cylindrical geometry with axial symmetry. Initial stress is proportional to the temperature distribution (equation (4)), and initial displacements are zero. The surface expands in response to the stress distribution. A maximum in surface displacement occurs 310 ns following absorption of the 8 ns pulse. This peak corresponds with the time needed for longitudinal acoustic waves from the beam edge, the 'hot–cold' boundary, to reach the centre.

The initial rising slope of the surface displacement curve (figure 2, $2000 < t < 2200$ ns) is determined by effective penetration depth and longitudinal sound speed ($D_{\text{eff}}$ and $c_L$). As described above, sound speed is found from the peak displacement, then effective penetration depth is used to fit the rising slope of the curve. We generate a unique numerical prediction that fits the experimental result using values of $c_L$ and $D_{\text{eff}}$. The uncertainty for the parameters used in the fit is $\pm 6$ m s$^{-1}$ for $c_L$ and $\pm 5$ $\mu$m for $D_{\text{eff}}$. The surface then falls to its quasi-steady state equilibrium value; 100 nm in figure 2. Equilibrium displacement, $S_0$, is linear with laser fluence (equation (7)). From a plot of equilibrium displacement versus fluence, the ratio of thermal expansion coefficient to heat capacity $\beta/C_V$, can be found as all other parameters in equation (7) are known.

As described earlier, we use a Poisson's ratio of $\nu = \frac{1}{2}$ for a hydrated sample such as meniscus. The geometrical correction factor $g_0(R)$ can be determined from the aspect ratio $R = w/D_{\text{eff}}$. We know the beam radius, and the effective penetration depth is found from the surface displacement curve. Thus, the Grüneisen coefficient, $\Gamma = c_L^2 \beta/C_V$, can be measured from the laser-induced response of a hydrated tissue such as knee meniscus. The equation of state of a solid, $P = \Gamma\varepsilon$, defines the Grüneisen coefficient as the ratio of pressure to energy density (Zemansky 1957).

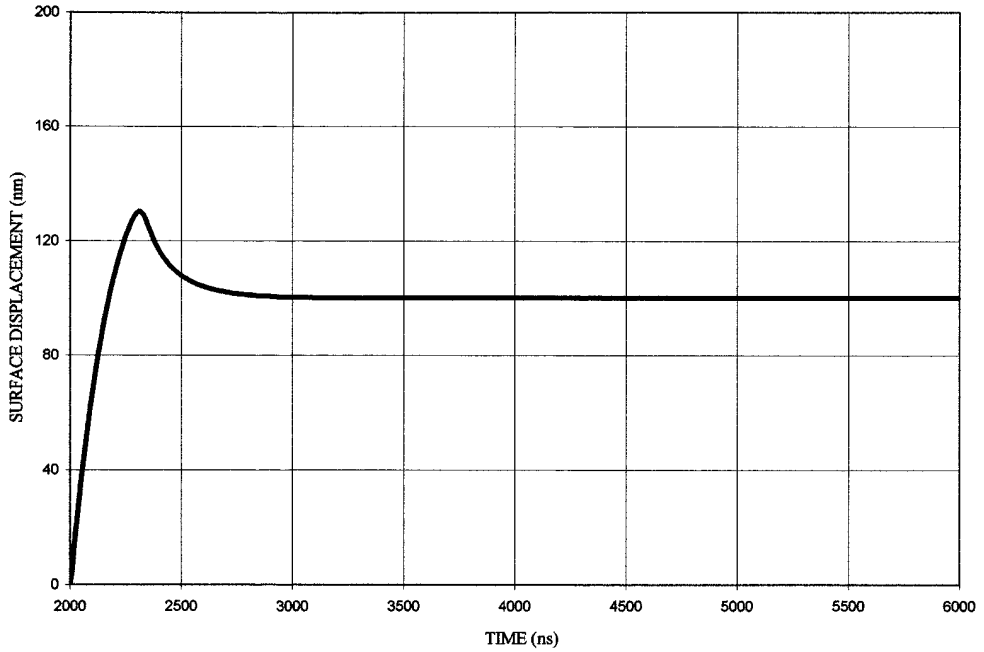


**Figure 2.** The predicted displacement of the surface of the centre of the irradiated disc ($r = 0$, $z = 0$) as a function of time. The following values were used: beam radius $w = 500$ $\mu$m, longitudinal sound speed $c_L = 1600$ m s$^{-1}$, penetration depth $D_{\text{eff}} = 350$ $\mu$m, Poisson ratio $\nu = \frac{1}{2}$.

## 3. Results

### *3.1. Verification of theory with gelatin experiments*

Gelatin, whose water content and optical absorption can be controlled, was used as an experimental model of a hydrated tissue. Following a laser pulse occurring at 2000 ns, gelatin behaves similarly to knee meniscus (compare with figure 5). Figure 3 shows the laser-induced surface displacement of a 20% gelatin sample. Data points between 0 and 2000 ns show that the gelatin surface is stationary, displacement is 0 nm. At 2000 ns, the laser fires, and the surface rises to a 200 nm maximum displacement at 2350 ns before reaching its equilibrium displacement (160 nm). The magnitude of thermoelastic expansion of a hydrated tissue to an 8 ns pulse is linear with laser fluence. Its time-dependent shape is constant, as demonstrated in figure 4; as the data are essentially normalized for laser fluence. Equilibrium displacement is normalized to a value of 1 for each fluence. For gelatin, the surface expansion reaches its peak at 2340 ns, which corresponds with the acoustic waves propagating to the centre from the 'hot–cold' boundary. For a pump beam radius of 0.51 mm, we obtain a longitudinal sound speed of

$$c_L = \frac{w}{t_{\text{peak}}} = \frac{0.51 \text{ mm}}{340 \text{ ns}} = 1500 \text{ m s}^{-1}. \tag{8}$$

This value is within 1% of the sound speed in water, and reasonable since our sample is composed of 80% water. The best fit to experiment is made using $D_{\text{eff}} = 500$ $\mu$m, $c_L = 1500$ m s$^{-1}$ and $\nu = \frac{1}{2}$. The value of Poisson's ratio, $\nu = \frac{1}{2}$, corresponds with the

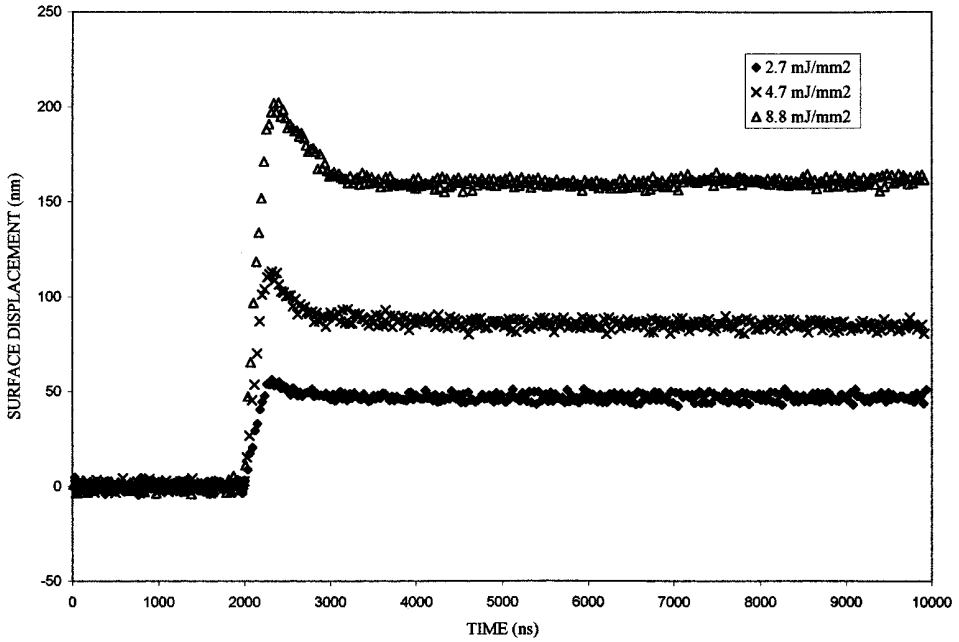


**Figure 3.** Surface displacement of 20% gelatin as a function of time as measured by laser surface interferometry. The Nd:YAG pulse fires at 2000 ns. The overall magnitude of the displacement increases with the value of laser fluence.

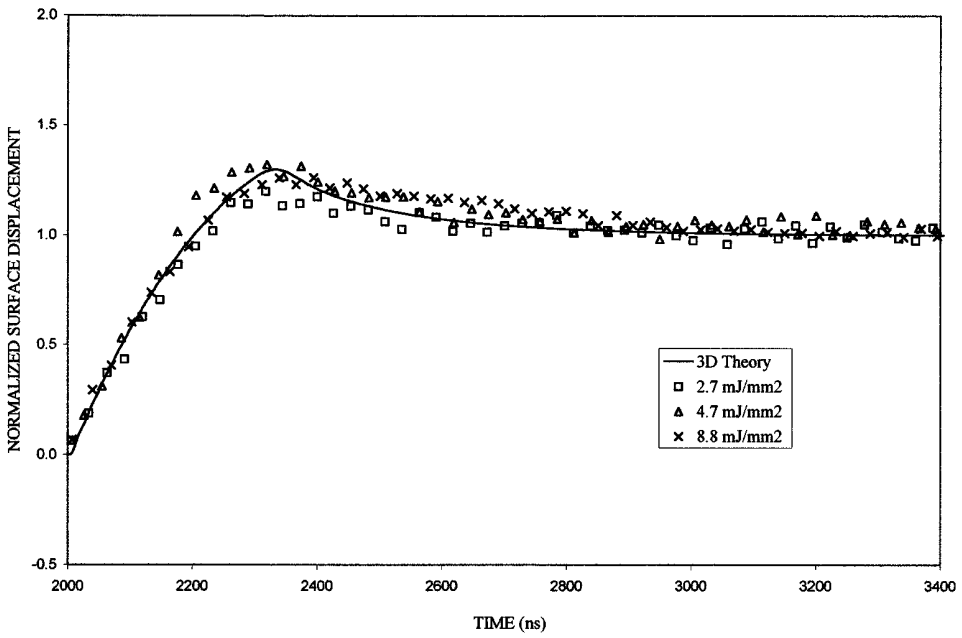


**Figure 4.** Normalized surface displacement of 20% gelatin. The surface displacement of gelatin, normalized to an equilibrium value of 1, agrees well with theoretical predictions. The time-dependent features are constant for different laser fluences. The best prediction is made using these values: $c_L = 1500$ m s$^{-1}$, $D_{\text{eff}} = 500$ $\mu$m, $\nu = \frac{1}{2}$.

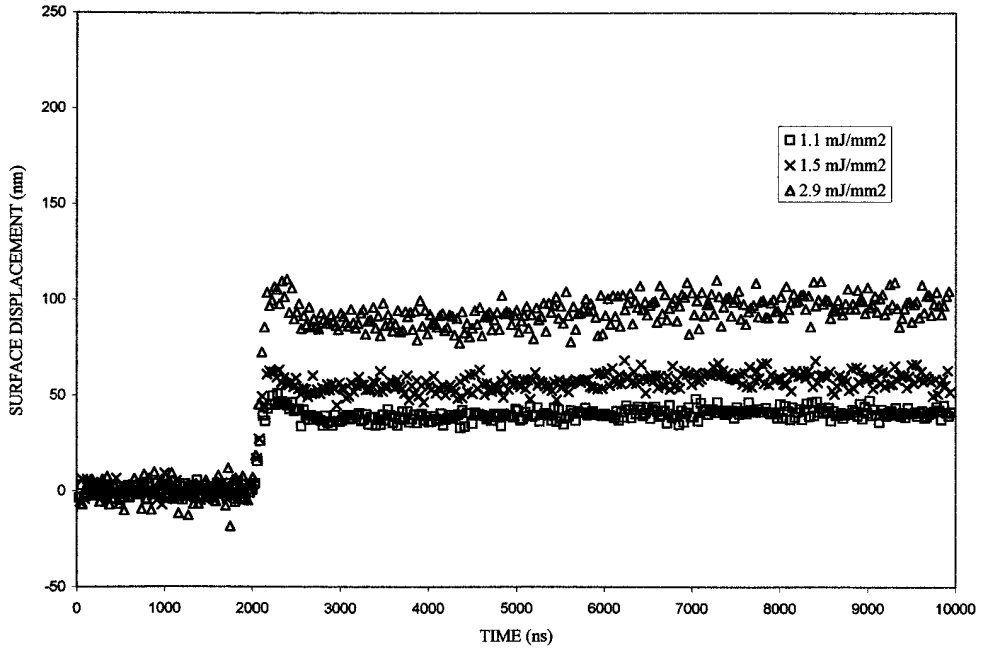


**Figure 5.** Surface displacement of human knee meniscus as a function of time as measured by laser surface interferometry. The laser pulse fires at 2000 ns.

fact that shear stress is not supported in this primarily water sample, and the transverse speed of sound is zero. We do not observe the second peak that was seen in hard samples, occurring when transverse waves from the beam edge reach the centre (Itzkan *et al* 1995).

### *3.2. Time-dependent thermoelastic behaviour of meniscus*

The surface displacement curve shape of meniscus is shown for several laser fluences (figure 5). The sample surface is initially stationary. It rises after absorption of the 8 ns pulse at 2000 ns, and reaches a peak that corresponds to longitudinal waves from the pump beam edge reaching the centred HeNe probe. The sample surface then falls to a quasi-steady state (QSS) equilibrium displacement, at which the surface will remain until thermal diffusion occurs. A typical meniscus sample reaches maximum expansion at 2330 ns, 330 ns following the pulse (figure 5). For a fluence of 2.9 mJ mm$^{-2}$, the surface approaches its equilibrium value of 90 nm. The best fit to these data (figure 6) using the numerical model was made using a sound speed of $c_L = 1600$ m s$^{-1}$ and effective penetration depth $D_{\text{eff}} = 280$ $\mu$m. For 22 meniscus samples, we found the mean values ($\pm$ standard deviation) of longitudinal sound speed and effective penetration depth at $\lambda = 355$ nm to be $\bar{c}_L = 1650$ ($\pm 70$) m s$^{-1}$ and $\bar{D}_{\text{eff}} = 253$ ($\pm 17$) $\mu$m.

### *3.3. Quasi-steady state equilibrium displacement of meniscus*

Figure 7 shows the equilibrium displacement versus laser fluence at four different sites on a meniscus sample. Equilibrium displacement is linear as a function of fluence, but varies between meniscus samples. Sample 4 shows approximately half the equilibrium displacement when compared with the other three sites irradiated with similar fluences. Using equation (7),

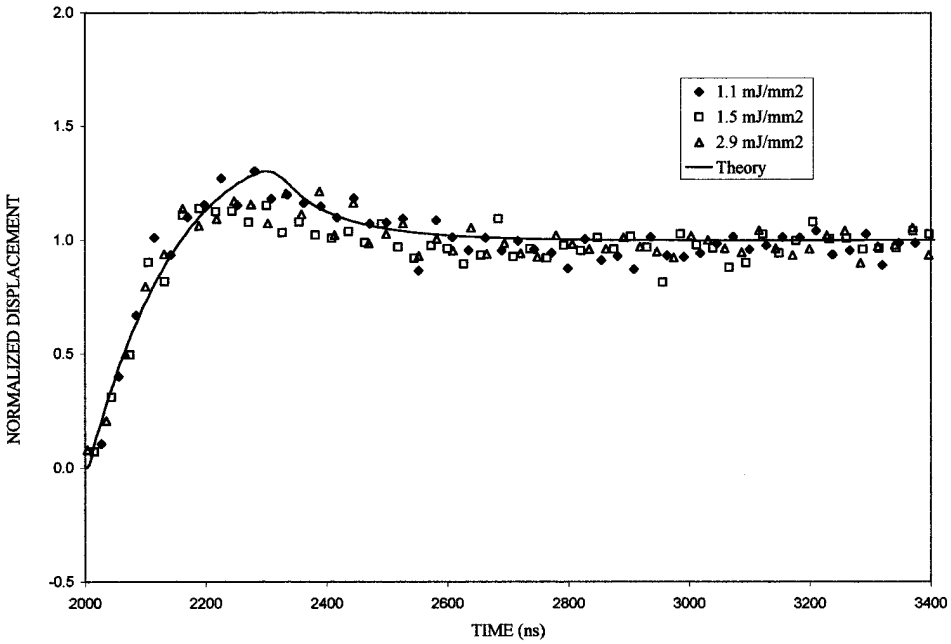


**Figure 6.** Normalized surface displacement of knee meniscus. Displacement, normalized to an equilibrium value of 1, agrees with theoretical predictions. Again, time-dependent features are constant with laser fluences. We used the following values for the theoretical prediction: $c_L = 1600$ m s$^{-1}$, $D_{\text{eff}} = 280$ $\mu$m, $\nu = \frac{1}{2}$.

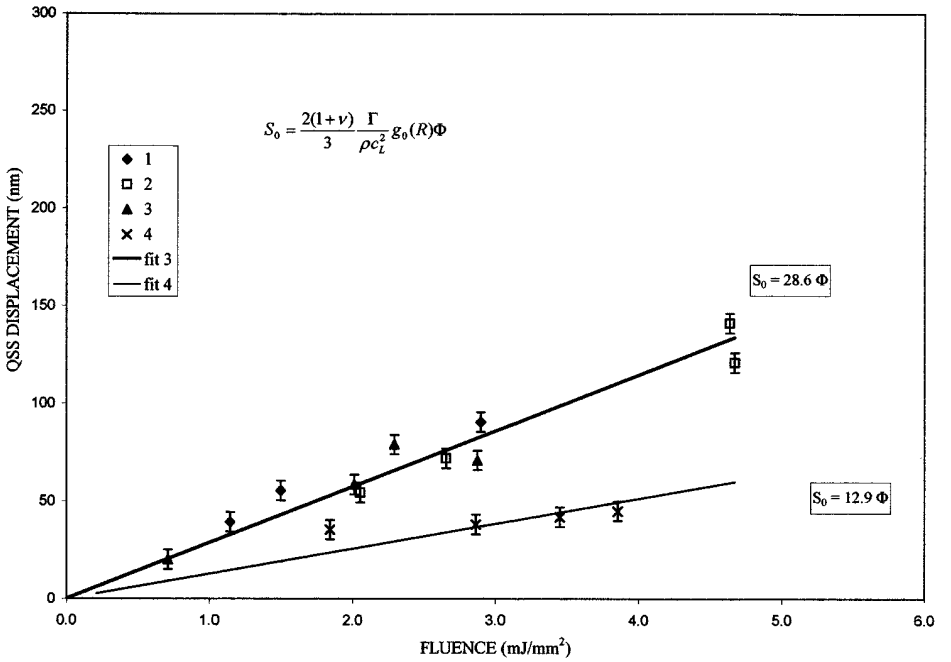


**Figure 7.** Quasi-steady state equilibrium of meniscus samples versus laser fluence. Three sites showed similar behaviour. The fourth shows approximately half the equilibrium displacement.

**Table 1.** Values of the Grüneisen coefficient for meniscus data (figure 7). Sample 4 has a lower value which corresponds to increased degenerative change (Dark 1999).

| Sample no. | Grüneisen coefficient $\Gamma$ |
|---|---|
| 1 | 0.15 |
| 2 | 0.13 |
| 3 | 0.13 |
| 4 | 0.057 |

the measured equilibrium displacement can be utilized as described above to determine the Grüneisen coefficient, $\Gamma$, of knee meniscus. For comparison, the higher values of Grüneisen coefficient denote the stronger tissue samples. For the samples of figure 7, values of the Grüneisen coefficient are given in table 1. The Grüneisen coefficient for 23 samples ranges from 0.057 to 0.21. As a comparison, the Grüneisen coefficient for bovine tibial bone is $\Gamma = 1.1$ (Duck 1990, Albagli 1994).

## 4. Discussion

Interferometric surface monitoring is an experimental technique that measures surface expansion of a material following irradiation by a nanosecond laser pulse. We use an initial light and temperature distribution that decays exponentially with an effective penetration depth. The non-zero temperature distribution results in laser-induced stresses and deformations that we can predict by numerically solving the thermoelastic wave equation.

By comparing measured surface expansion and theoretical predictions, one can obtain the longitudinal sound speed, optical penetration depth and the Grüneisen coefficient of knee meniscus. The longitudinal sound speed of meniscus is greater than that of water by approximately 10%, which is reasonable since meniscus is composed mainly of water. The effective penetration depth of meniscus at $\lambda = 355$ nm is $D_{\text{eff}} = 253$ $\mu$m. This value for effective penetration depth of meniscus at $\lambda = 355$ nm compared well with previous spectrophotometer measurements made by our group (Dark 1999). Grüneisen coefficient ranges from 0.057 to 0.21. A comparison of the value of Grüneisen coefficient to an evaluation of the tissue's condition may be useful as a potential method for diagnosing degenerative changes in knee meniscal tissue.

## Acknowledgments

The authors wish to thank Dr Maryann Fitzmaurice who performed the histological assessment of the menisci, and the orthopaedic nursing staff who assisted with the collection of tissue samples. Our work at the MIT Laser Biomedical Research Center was supported by grant P41-RR 02594 from the National Institute of Health.

## References

Adams M E and Hukins D W L 1992 The extracellular matrix of the meniscus ed V C Mow, S P Arnoczky and D W Jackson *Knee Meniscus: Basic and Clinical Foundations* (New York: Raven) pp 15–28

Albagli D 1994 Fundamental mechanisms of pulsed laser ablation of biological tissue *PhD Thesis* Massachusetts Institute of Technology

Albagli D, Dark M, Perelman L T, von Rosenberg C, Itzkan I and Feld M S 1994a Photomechanical basis of laser ablation of biological tissue *Opt. Lett.* **19** 1684–6

Albagli D, Dark M, von Rosenberg C, Perelman L T, Itzkan I and Feld M S 1994b Laser-induced thermoelastic deformation: a three dimensional solution and its application to the ablation of biological tissue *Med. Phys.* **21** 1323–31

Bullough P G 1992 *Atlas of Orthopedic Pathology* (New York: Gower Medical)

Dark M L 1999 The physical response of soft musculoskeletal tissues to short pulsed laser irradiation *PhD Thesis* Massachusetts Institute of Technology

Duck F A 1990 *Physical Properties of Tissue* (London: Academic)

Ghosh P and Taylor T K F 1987 The knee joint meniscus *Clin. Orthop.* **224** 52–63

Itzkan I, Albagli D, Dark M L, Perelman L T, von Rosenberg C and Feld M S 1995 The thermoelastic basis of short pulsed laser ablation of biological tissue *Proc. Natl Acad. Sci. USA* **92** 1960–4

Landau L D and Lifshitz E M 1986 *Theory of Elasticity* 3rd edn (Oxford: Pergamon)

Oraevsky A A, Jacques S L, Esenaliev R O and Tittel F K 1996 Pulsed laser ablation of soft tissues, gels and aqueous solutions at temperatures below 100 °C *Lasers Surg. Med.* **18** 231–40

Paltauf G and Schmidt-Kloiber H 1996 Microcavity dynamics during laser-induced spallation of liquids and gels *Appl. Phys.* A **62** 303–11

Potter D 1977 *Computational Physics* (New York: Wiley)

Schaffer J L, Dark M L, Itzkan I, Albagli D, Perelman L T, von Rosenberg C and Feld M S 1995 Mechanisms of meniscal tissue ablation by short pulse laser irradiation *Clin. Orthop.* **310** 30–6

Star W M 1995 Diffusion theory of light transport *Optical-Thermal Response of Laser-Irradiated Tissue* ed A J Welch and M J C van Gemert (New York: Plenum)

Yablon A D, Nishioka N S, Mikic B B and Venugopalan V 1999 Measurement of tissue absorption coefficients by use of interferometric photothermal spectroscopy *Appl. Opt.* **38** 1259–72

Zemansky M W 1957 *Heat and Thermodynamics* (New York: McGraw-Hill)